Enhanced Photocatalytic Hydrogen Production Under Visible Light over Ag Doped TiO_2

V. Guzmán-Velderrain[1], M. Meléndez Zaragoza[1], E. Medina-Henandez[2], P. Gutiérrez Rivera[3], Y. Ortega-López[1], J. Salinas Gutiérrez[1], A. López Ortiz[1], V. Collins-Martínez[1*]

[1]Centro de Investigación en Materiales Avanzados S. C., Laboratorio Nacional de Nanotecnología, Depto. de Materiales Nanoestructurados, Miguel de Cervantes 120, C. P. 31109, Chihuahua, Chih. México
[2]Universidad Autónoma de Chihuahua, Facultad de Ciencias Químicas, Campus Universitario # 2 C.P. 31125, Chihuahua, Chih, México
[3]Universidad Tecnología Junta de los Ríos, Carretera Aldama, Km 3, C. P. 31313, Chihuahua, Chih. México
* Tel: +52 (614)439 11 29, e-mail: virginia.collins@cimav.edu.mx

ABSTRACT

TiO_2 is the most widely used photocatalyst for water and air purification, and for hydrogen production, due to its good properties such as chemical and photo-corrosion resistance and low cost. One disadvantage of this material, resides in its bandgap energy (3.2eV), which lies in the UV spectrum. For this reason, studies have been conducted to modify TiO_2 bandgap into the visible light range. Doping elements used for this purpose are noble metals such as Au, Pt and Ag. However, Au and Pt are expensive and scarce materials, leaving Ag as a preferred candidate. TiO_2 and doped TiO_2 were synthesized via sol-gel/hydrothermal (SGH) named TiO_2-F and TiO_2Ag-F, respectively, while under the sol-gel/hydrothermal/thermal (SGHT) technique was named as TiO_2Ag-C, using titanium butoxide as a precursor and ethanol as solvent. XRD characterization resulted in the presence of the anatase phase in all three synthesized samples as well as the characteristic signals for metallic Ag in TiO_2Ag-F. Samples crystal sizes were determined by the Scherrer equation, and were ~ 10 nm. Light absorption exhibited a shift in the Eg value from 3.05 eV for TiO_2-F to 2.8 eV for TiO_2Ag-F. BET surface area for the SGH and SGHT photocatalysts were of 140 and 95m^2/g, respectively. SEM images presented particle agglomerates of irregular morphology. Photocatalytic evaluation for hydrogen production was performed using a 250 W mercury light lamp, filtering the UV spectrum. TiO_2Ag-F was the only sample that showed activity, producing 180 µmol of H_2/g catalyst over a 4h irradiation period. This activity can be mainly attributed to the ability of this material to be activated under the visible light spectrum and to the silver in a metallic state in TiO_2, which inhibits the recombination of the electron-hole pair generated when the material is activated under light exposure.

Keywords: TiO_2 doped Ag;, Water splitting; Hydrothermal method.

1. Introduction

Today, the main source of energy in most countries, is based on the burning of fossil fuels, which increases each year due to population growth and daily activities. One concern about the excessive use of this source of energy is the amount of pollutants released into the atmosphere, which causes the greenhouse effect and the increase in earth temperature (global warming) [1, 2]. Due to this problem it is important to make use of alternative energy sources such as wind, biomass, nuclear [3] hydrothermal, geothermal and solar [4]. A disadvantage of these type of energy sources are their low efficiency, hence another energy alternative is through fuel cells and hydrogen. Hydrogen obtained through the separation of the water molecule (water splitting), promises to replace fossil fuels as a source of clean energy without the emission of pollutants and greenhouse gases such as CO_2, CO, SO_x, NO_x [5, 6]. By the breakthrough discovery of molecular water splitting, several processes have been developed, among them the photocatalytic. Research interest in hydrogen production via photocatalysis focuses primarily on the study of efficient semiconductor materials under the sunlight spectrum [7].

Titanium dioxide (TiO_2) is one of the most widely used photocatalyst in recent years, some of its uses have been in the degradation of toxic organic pollutants in both water and air and in the dissociation of the water molecule. Main advantages of this photocatalyst reside in its strong resistance to a wide variety of chemicals, as well as to the photocorrosion, besides its low cost [8]. However, a drawback to this material is that it has a band gap value (band gap) in the range of the ultraviolet light (3.2 eV), which within the solar spectrum extents to only 4%. Therefore, its activity is negligible under visible light irradiation and consequently its application is limited [9]. For this reason, studies have been conducted to reduce the bandwidth of TiO_2 into the visible light range through its doping. Among the elements that have been used for this purpose are; noble metals such as gold, platinum and silver (Au, Pt and Ag). Although gold and platinum provide good results towards the decrease of the bandgap, these are very expensive and scarce materials, so that silver can be considered as a potential candidate, because of lower cost and greater accessibility. Several studies where TiO_2 is doped with silver in various fields of application are reported; degradation of dyes (methyl orange, methyl red and crystal violet) as well as the hydrogen production via photocatalysis [10].

The objective of the present work is to synthesize crystalline TiO_2 powders at low temperature doped with silver, to observe the effect of the dopant material on the modification of its band gap, as well as to evaluate the photocatalytic activity towards hydrogen production in the range of visible light.

2. Experimental

2.1. Precursor solutions synthesis

Precursor solutions for doped and undoped TiO_2 powders were prepared by the Sol-Gel/Hydrothermal technique. For the sol-gel synthesis titanium n-butoxide, (ACROS trademark) with a purity of 99% was used as precursor, while for Ag, silver nitrate ($AgNO_3$, DEQ trademark) 99.8%, was employed as precursor and mixed in a 4.5% Ag/TiO_2 a molar ratio and this was dissolved in 5.08 ml of ethanol, 6.44 ml of acetic acid and 0.88 ml of water. A second solution with 8 ml of ethanol and 5.44 ml of titanium

butoxide was also prepared. Both solutions were mixed to form a final solution, which was kept under stirring for 1h. Subsequently, these solutions were subjected to a hydrothermal process at 200 ° C for 2h and finally one of the samples was exposed to a thermal treatment at 200 °C for 3h.

The nomenclature used for the different synthesized samples is presented in Table 1.

Table 1. Nomenclature of synthesized samples

Sample	Doping	Treatment	Temperature °C
TiO_2-F	N/A	Hydrothermal	200
TiO_2Ag-F	4.5%Ag	Hydrothermal	200
TiO_2Ag-C	4.5%Ag	Hydrothermal/Thermal	200/200

2.2. Characterization of Materials

TiO_2 powders were characterized by different techniques, with the aim of studying their physical and chemical features. To determine the crystal structure present in the materials, the powders were analyzed by XRD, using an XPert Pro diffractometer with a wavelength of 1.5406Å and between 15 to 85 ° in 2θ, with a step size of 0.05 and 120s by step. The crystal size of the samples using was calculated by the Scherrer's equation. To obtain the light absorption spectra of the materials the UV/Vis spectroscopy technique was employed, using a Perkin Elmer spectrophotometer (lamda-10) equipped with integrating sphere for diffuse reflectance studies. The particle size of the powders were determined by ultra-high resolution transmission electron microscopy (MET) using a JEM-2200FS that combines an emission gun of 200 kv with an omega filter and equipped with a system for energy dispersive spectroscopy (EDS) for elemental analysis of samples. The surface area of the powders was evaluated by the technique of nitrogen physisorption (BET) to a degassing temperature of 180 ° C, using a Quantachrome Autosorb-1.

2.3. Photocatalytic Evaluation

200 mg of the synthesized TiO_2 powders were suspended in water and methanol, the latter was used as a sacrificial agent; The suspension was placed inside a quartz batch type photoreactor (Figure 1) with a length of 19 cm and a diameter of 5 cm, which was sealed and located 7 cm away from a mercury lamp of 250 W in which 200 ml of distilled water, 4 ml of methanol and 0.2 g of photocatalyst were loaded, all under constant stirring and under illumination for 4h. Hydrogen production was monitored by gas chromatography using a gas chromatograph Perkin Elmer Clarus 500.

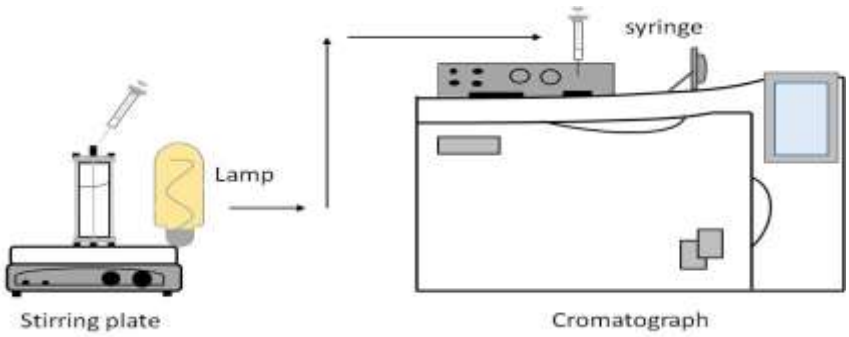

Fig 1. Photocatalytic process evaluation diagram.

3. Results and discussion

3.1. X ray Diffraction

XRD patterns of synthesized undoped and Ag-doped TiO_2 photocatalysts under different treatment conditions are presented in Figure 2. In these diffraction patterns it can be observed main reflections that belong to the anatase phase (characteristic signals (101) at 25° and (004) to 37.8° in 2θ) [11]. However, for TiO_2Ag-F sample a reflection peak at 38.2° in 2θ belonging to the (111) silver can be seen, overlapping with the signal (004) of anatase, reason why this presents a greater intensity in this pattern, besides the presence of the peak at 2θ 44.32° that corresponds to the (200) reflection, confirming the existence of metallic silver in the cubic phase sample [12]. This result can be explained considering that during the sol-gel process, silver was not incorporated into the TiO_2 crystal lattice, producing silver oxide and after review of the thermodynamic data, when this oxide is exposed to the temperature of the hydrothermal process (200 °C) this is converted to metallic silver. While in TiO_2Ag-C sample by applying a heat treatment silver atoms are driven to migrate towards the TiO_2 lattice, thus achieving their entire incorporation into TiO_2 causing silver reflections to disappear [13].

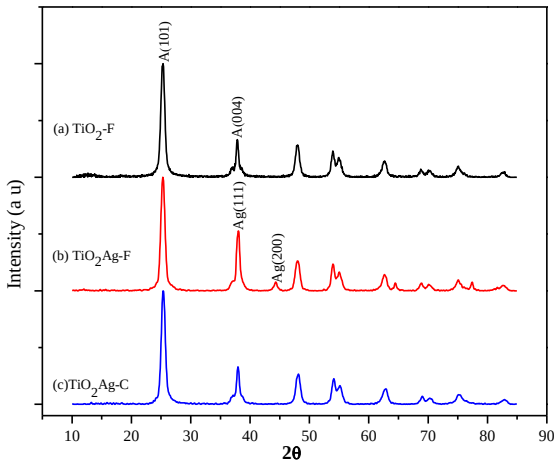

Fig 2. Diffraction patterns of TiO_2-F(a), TiO_2Ag-F(b) and TiO_2Ag-C(c)

3.2. Crystal Size

Table 2 presents calculated crystal sizes obtained from the Scherrer's equation and the diffraction patterns of each material. The synthesized materials present crystal size values of 10.4, 9.8 and 10.1 nm corresponding to the TiO_2-F, and TiO_2Ag TiO_2Ag-C-F samples, respectively. The reduction the crystal size for sample TiO_2Ag-F is associated with the previous explanation: during the sol-gel the Ag^+ ions are converted to silver oxide, so that the later during the hydrothermal treatment are transformed into elemental silver resulting in a physical barrier between the TiO_2 nanocrystals. This phenomenon causes the required movement for the crystals to reach its densifying energy and thereby the growth of these crystals is inhibited [14, 15, 16, 17]. Furthermore, the TiO_2Ag-C sample shows a slight increase in crystal size that can be attributed to crystal growth caused by the heat treatment to which the material was exposed.

Table 2. Estimated crystal size using the Scherrer's equation

Sample	Crystal Size (nm)
TiO_2-F	10.4
TiO_2Ag-F	9.8
TiO_2Ag-C	10.1

3.3. UV-Vis Spectra

Diffuse reflectance spectra (UV-Vis) for doped and undoped TiO_2 in Kubelka Munk units are presented in Figure 3. In order to determine the sample band gap the linear inflection region of the diffuse reflectance spectrum was considered, which represents the energy absorption over the edge. Extrapolating the slope of the linear region to intercept the photon energy axis (x-axis), this point provides the value of optical band gap of the material.

For the spectrum of sample TiO_2-F the estimated value of the energy band gap was ~ 3.05 eV, which is within the reported values of TiO_2 in anatase phase ranging from 3.05 to 3.2eV and outside the visible light spectrum [18].

By doping TiO_2 with Ag, the samples show a decrease in the bandgap. The value obtained for the doped sample TiO_2Ag-F corresponds to 2.8eV. This change in band gap energy is greatly attributed to the localized surface plasmon resonance (465 nm) generated by Ag nanoparticles; the presence of Ag on the surface of titanium oxide drastically creates a disturbance in the dielectric constant of the surrounding matrix and contributes for the material to be able to absorb visible light [19]. While the band gap value for TiO_2Ag-C sample was 2.6eV. This absorption shift towards red ~ 0.5 eV (62 nm) is attributable to the dopant metal, which generate energy states located above the valence band [20].

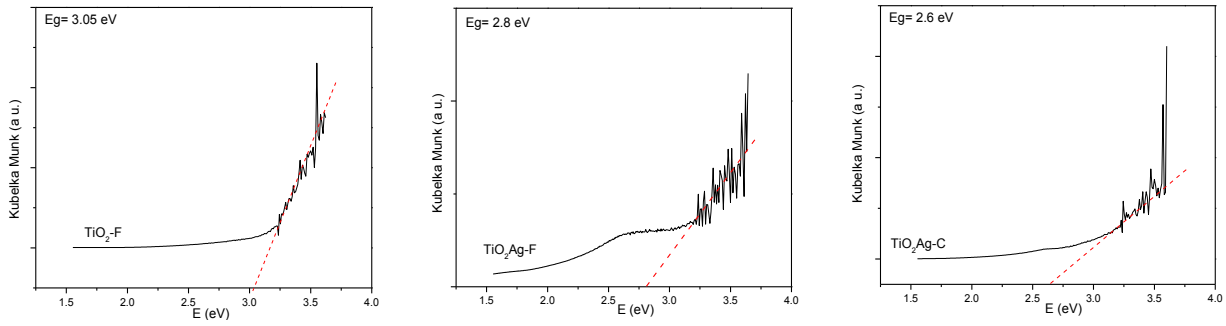

Fig 3. UV-Vis Diffuse Reflectance Spectra for the TiO_2-F TiO_2Ag-F and TiO_2Ag-C samples

3.4. Transmission electron microscopy

Transmission electron microscopy images for the synthesized samples are presented in Figure 4. Morphology of the samples consist in agglomerates of ellipsoid particles of nanometer size. The average particle size was determined by a statistical calculation of the average diameter of about 100 particles. The estimated particle size for the samples was between 12 and 18 nm, as presented in Table 3. Larger particle sizes were exhibited by sample TiO_2-F and this is due to the fact that during the nucleation and growth of the crystals these do not have the presence of the physical barrier of silver. Moreover, image analysis by Energy Dispersive Spectroscopy (EDS) of the TiO_2Ag-F sample, present free silver particles, confirming the results obtained by X-ray

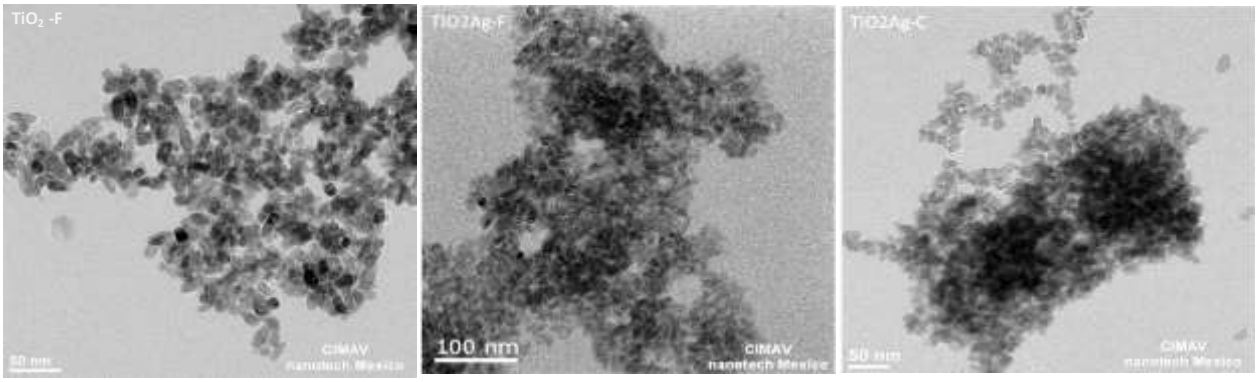

Fig 4. TEM images for the TiO_2-F (a) and TiO_2Ag-F (b) and TiO_2Ag-C (c) sample powders

3.5. BET Surface Area

The specific surface area for each photocatalyst was determined by N_2 physisorption and they were; 124, 138 and 93 m^2/g for TiO_2F, TiO_2Ag and TiO_2Ag-F-C, respectively. These results were expected since the present synthesis method is used to produce nanoparticles and consequently the effect of high surface areas is reflected. Likewise, it can be seen that when doping titanium with silver and after applying only

the hydrothermal treatment, an increase in surface area is reached. This is because the size of the crystal is decreased (as shown and explained in the crystal size section), which causes a decrease in particle size and an increase in surface area. Furthermore, it is noted that the TiO_2Ag-C sample has a reduced surface area and increased particle size. This is associated with this material suffering a sintering process caused by the heat treatment to which this sample was exposed.

Table 3. Surface area and particle size for the synthesized TiO_2 powders

Sample	Area (m^2/g)	Particle Size (nm)
TiO_2-F	125	18
TiO_2Ag-F	140	12
TiO_2Ag-C	95	15

3.6. Photocatalytic Evaluation

Evaluation of the photocatalytic activity for the different synthesized samples by the hydrogen evolution produced by the splitting reaction of the water molecule via photocatalysis is presented in Table 4. Results indicate that the H_2 production that was achieved after 4h irradiation presented the following order TiO_2Ag-F-C > TiO_2Ag > TiO_2-F. This behavior can be explained with the fact that TiO_2 samples that present an increased H_2 production are those doped with Ag, and these being active under the visible light spectrum, this also explains the low H_2 production of undoped TiO_2, as its activation energy is located in the UV region. On the other hand, differences in the performance of silver doped TiO_2 can be explained with studies reported by J. Yu et al. [19]. When silver is present in metallic form (as in the case of TiO_2Ag-F sample), additionally to helping reduce the bandgap through the interaction between the TiO_2-Ag phases, the electrons when excited from the valence band to the conduction band migrate to the Ag clusters, thus preventing the direct recombination of electrons and holes (a large disadvantage that TiO_2 has). When silver is incorporated into the TiO_2 crystal lattice (TiO_2Ag-C), only enter the intermediate states to decrease the bandgap energy, leaving the TiO_2 with its problem; a very fast recombination of electron-hole pair, which is reflected in the low production of H_2.

Table 4. Hydrogen production by the synthesized photocatalysts

Sample	$\mu moles H_2/g_{cat}$
TiO_2-F	15
TiO_2Ag-F	180
TiO_2Ag-C	30

4. Summary and perspectives

- In the present work, it was possible to synthesize undoped and silver doped TiO_2 through the sol-gel assisted hydrothermal treatment.

- X-ray results showed that TiO_2 presents only the anatase phase in all samples. For the doped samples, superficial metallic silver results when the hydrothermal treatment is only applied and by temperature effect (thermal treatment) silver incorporation into TiO_2 lattice is achieved.
- TiO_2 crystal size is affected by metallic silver, which acts as a physical barrier to inhibit the growth of anatase crystals because 10.4nm of sample TiO_2-F is reduced to 9.8nm in sample TiO_2Ag-F and in 10.1nm of sample TiO_2Ag-C. The morphology presented in TiO_2 samples was of ellipsoidal nanoparticles with an average particle size of 18 nm for TiO_2-F and 12 and 15 nm for TiO_2Ag-F and TiO_2Ag-C samples, respectively. Surface areas exhibited by the synthesized samples were affected by the particle size of the materials and these were: 125, 140 and 95 m^2/g for TiO_2-F, TiO_2Ag-F and TiO_2Ag-C, respectively.
- The value of the energy bandgap found for anatase 3.05 eV agrees with that reported in the literature. The shifting to red that silver induce in the TiO_2 bandgap is according to how silver is incorporated into this; when the effect is by interaction between phases (TiO_2-Ag°) as in the case of TiO_2Ag-F this is of 2.8 eV, and when Ag enters the lattice generating the intermediate states as shown in TiO_2Ag-C is of 2.6 eV, since both TiO_2 doped samples were active under the visible light spectrum.
- H_2 production achieved after 4 hours of light irradiation had the following order: TiO_2Ag-F>TiO_2Ag-C-F>TiO_2. The maximum H_2 production was of 180 µmol H_2/g_{cat}. The inhibition in recombination of the electron-hole pair that produce Ag metallic clusters in TiO_2, when attracting electrons, is decisive in the photocatalytic activity of these materials towards the dissociation of the water molecule for H_2 production.

Acknowledgements

The authors thank technicians: Teresa María Chaparro, Enrique Torres, Luis de la Torre and Carlos Ornelas for their contributions to the UV-Vis spectroscopy, BET, X-ray diffraction and scanning electron microscopy results. As well as the Centro de Investigación en Materiales Avanzados for their support in the use of its infrastructure.

References

[1] N. Naseri, H. Kim, W. Choi, A.Z. Moshfegh Optimal Ag concentration for H_2 production via Ag:TiO_2 nanocomposite thin film photoanode international journal of hydrogen energy 37 (2012) 3056e3065.

[2] M. Davoudi, M.R. Rahimpour, S.M. Jokar, F. Nikbakht, H. Abbasfard The major sources of gas flaring and air contamination in the natural gas processing plants: A case study Journal of Natural Gas, Science and Engineering 13 (2013) 7e19.

[3] Manuel Frondel, Nolan Ritter, Christoph M. Schmidt, ColinVance Economic impacts from the promotion of renewable energy technologies: The German experience Energy Policy 38 (2010) 4048–4056.

[4] Ayhan Demirbas Potential applications of renewable energy sources, biomass combustion problems in boiler power systems and combustión related environmental issues Progress in Energy and Combustion Science 31 (2005) 171–192

[5] Surakerk Onsuratoom, Sumaeth Chavadej, Thammanoon Sreethawong Hydrogen production from water splitting under UV light irradiation over Ag-loaded mesoporous-assembled TiO_2–ZrO_2 mixed oxide nanocrystal photocatalysts international journal of hydrogen energy 36 (2011) 5246-5261

[6] Stéphane Abanades, Patrice Charvin, Gilles Flamant, Pierre Neveu Screening of water-splitting thermochemical cycles potentially attractive for hydrogen production by concentrated solar energy Energy 31 (2006) 2805–2822.

[7] Honghui Yang, Liejin Guoa, Wei Yan, Hongtan Liu, A novel composite photocatalyst for water splitting hydrogen production, Journal of Power Sources 159 (2006) 1305–1309.

[8] K. Kocˇi, K. Mateˇju˚ , L. Obalova, S. Krejcˇikova, Z. Lacny´, D. Placha, L. Cˇapek, A. Hospodkova, O. ˇSolcova Effect of silver doping on the TiO_2 for photocatalytic reduction of CO_2, Applied Catalysis B: Environmental 96 (2010) 239–244.

[9] Ali Akbar Ashkarran, Habib Hamidinezhad, Hedayat Haddadi, Morteza Mahmoudi, Double-doped TiO_2 nanoparticles as an efficient visible-light-active photocatalyst and antibacterial agent under solar simulated lightApplied Surface Science 301 (2014) 338–345.

[10] Kenneth J. Klabunde, Dambar B. Hamal, Synthesis, characterization, and visible light activity of new nanoparticle photocatalysts based on silver, carbon, and sulfur-doped TiO_2, Journal of Colloid and Interface Science 311 (2007) 514–522

[11] O.-Bong Yanga, M. Alam Khana, Seong Ihl Woob Hydrothermally stabilized Fe(III) doped titania active under visible light for water splitting reaction international journal of hydrogen energy 33 (2008) 5345–5351

[12] Kiran Gupta, R. P. Singh, Ashutosh Pandey and Anjana Pandey Photocatalytic antibacterial performance of TiO_2 and Ag-doped TiO_2 against S. aureus. P. aeruginosa and E. coli, Beilstein J. Nanotechnol. 2013, 4, 345–351

[13] Chao He, Yun Yu, Xingfang Hu, André Larbot Influence of silver doping on the photcatalytic activity of titania fims Applied Surface science 200 (2002) 239-247.

[14] .I.Y. Tok, S.W. Du, F.Y.C. Boey, W.K. Chong Hydrothermal synthesis and characterization of rare earth doped ceria nanoparticles Materials Science and Engineering A. 466 (2007) 223–229

[15] Chao He, Yun Yu, Xingfang Hu, André Larbot Influence of silver doping on the photcatalytic activity of titania fims Applied Surface science 200 (2002) 239-247

[16] Yongsong Cao, Huihua Tan, Tianyu Shi, Tao Tang and Jianqiang Li Preparation of Ag-doped TiO_2 nanoparticles for photocatalytic degradation of acetamiprid in water Journal of Chemical Technology and Biotechnology 83:546–552 (2008),

[17] Yuanpeng Gao, Pengfei Fang, Feitai Chen, Yang Liu, Zhi Liu, Dahai Wang, Yiqun Dai Enhancement of stability of N-doped TiO_2 photocatalysts with Ag loading Applied Surface Science 265 (2013) 796– 801.

[18] Deanna C. Hurum, Alexander G. Agrios, and Kimberly A. Gray Explaining the Enhanced Photocatalytic Activity of Degussa P25 Mixed-Phase TiO_2 Using EPR J. Phys. Chem. B 2003, 107, 4545-4549

[19] Jiaguo Yu, Jianfeng Xiong, Bei Cheng, Shengwei Liu Fabrication and characterization of Ag–TiO_2 multiphase nanocomposite thin films with enhanced photocatalytic activity Applied Catalysis B: Environmental 60 (2005) 211–221.

[20] Roshan Nainan, Pragati Thakur and Manohar Chaskar Synthesis of Silver Doped TiO_2 Nanoparticles for the Improved Photocatalytic Degradation of Methyl Orange Journal of Materials Science and Engineering B 2 (1) (2012) 52-58.